THE JOURNAL OF BIOLOGICAL CHEMISTRY
Vol. 280, No. 8, Issue of February 25, pp. 6960–6968, 2005

Printed in U.S.A.

The Heteromeric Organic Solute Transporter α-β, Ostα-Ostβ, Is an Ileal Basolateral Bile Acid Transporter*[S]

Received for publication, November 10, 2004, and in revised form, November 23, 2004
Published, JBC Papers in Press, November 24, 2004, DOI 10.1074/jbc.M412752200

Paul A. Dawson‡§, Melissa Hubbert‡, Jamie Haywood‡, Ann L. Craddock‡, Noa Zerangue¶, Whitney V. Christian‖, and Nazzareno Ballatori‖

From the ‡Departments of Internal Medicine and Pathology, Wake Forest University School of Medicine, Winston-Salem, North Carolina 27157, ¶XenoPort, Inc., Santa Clara, California 95051, and ‖Department of Environmental Medicine, University of Rochester School of Medicine, Rochester, New York 14642

Bile acids are transported across the ileal enterocyte brush border membrane by the well characterized apical sodium-dependent bile acid transporter (Asbt) *Slc10a2*; however, the carrier(s) responsible for transporting bile acids across the ileocyte basolateral membrane into the portal circulation have not been fully identified. Transcriptional profiling of wild type and *Slc10a2* null mice was employed to identify a new candidate basolateral bile acid carrier, the heteromeric organic solute transporter (Ost)α-Ostβ. By Northern blot analysis, Ostα and Ostβ mRNA was detected only in mouse kidney and intestine, mirroring the horizontal gradient of expression of Asbt in the gastrointestinal tract. Analysis of Ostα and Ostβ protein expression by immunohistochemistry localized both subunits to the basolateral surface of the mouse ileal enterocyte. The transport properties of Ostα-Ostβ were analyzed in stably transfected Madin-Darby canine kidney cells. Co-expression of mouse Ostα-Ostβ, but not the individual subunits, stimulated Na^+-independent bile acid uptake and the apical-to-basolateral transport of taurocholate. In contrast, basolateral-to-apical transport was not affected by Ostα-Ostβ expression. Co-expression of Ostα and Ostβ was required to convert the Ostα subunit to a mature glycosylated endoglycosidase H-resistant form, suggesting that co-expression facilitates the trafficking of Ostα through the Golgi apparatus. Immunolocalization studies showed that co-expression was necessary for plasma membrane expression of both Ostα and Ostβ. These results demonstrate that the mouse Ostα-Ostβ heteromeric transporter is a basolateral bile acid carrier and may be responsible for bile acid efflux in ileum and other ASBT-expressing tissues.

Bile acids are synthesized from cholesterol in the liver and secreted into the small intestine where they facilitate the absorption of dietary lipids and fat-soluble vitamins. The majority of bile acids are reabsorbed from the intestine, returned to the liver via the portal venous circulation, and resecreted into bile (1). The major mechanism for intestinal absorption is active transport by the well characterized ileal apical sodium bile acid co-transporter (ASBT,[1] gene name *Slc10a2*) (3, 4) in the distal ileum. Loss-of-function mutations in the human ASBT gene are associated with intestinal bile acid malabsorption (2), and targeted deletion of the ASBT gene eliminates enterohepatic cycling of bile acids in mice (3). Following their ASBT-mediated transport across the apical brush border membrane, bile acids are shuttled to the basolateral membrane and secreted into the portal circulation.

In contrast to apical transport, there is limited information regarding the ileal basolateral bile acid transporter. Using rat ileal basolateral membrane vesicles, bile acid transport was trans-stimulated by sulfate, bicarbonate ions, and *p*-aminohippurate, suggesting a sodium-independent anion exchange mechanism (4). Subsequent affinity labeling using tritiated bile acid photoprobes and subcellular fractionation studies implicated a 54-kDa protein enriched in the basolateral membrane (5–7); however no specific transporter was identified. Possible mechanisms for basolateral bile acid transport include a dedicated transporter, multiple transporters with broad substrate specificity that includes bile acids, or a combination of both systems. Considering the high flux of bile acids across the ileal enterocyte (1), it is likely that a dedicated basolateral bile acid transporter is required. More recently, additional candidate ileal basolateral bile acid transporters have been proposed, including t-Asbt (8) and the multidrug resistance-associated protein 3 (Mrp3, gene name *Abcc3*) (9, 10). However, their specific roles are uncertain, and the identity of the basolateral bile acid transporter remains a missing link in our understanding of the enterohepatic circulation. In this study, transcriptional profiling in *Slc10a2* null mice was used to identify a novel candidate ileal basolateral bile acid transporter.

EXPERIMENTAL PROCEDURES

Materials—[^{3}H]Taurocholic acid (2.0–3.0 Ci/mmol) was purchased from PerkinElmer Life Sciences. Inulin [^{14}C]carboxylic acid (2–10 mCi/mmol) and [^{32}P]dCTP (3000 Ci/mmol) were purchased from Amersham Biosciences. HEK293 (CRL-1573) and MDCK (CCL-34) cells were obtained from the American Type Culture Collection and grown in monolayer at 37 °C in an atmosphere of 5% CO_2. HEK293 cells were maintained in medium A consisting of Dulbecco's modified Eagle's medium containing 4,500 mg/liter D-glucose, 10% (v/v) fetal calf serum, and

* This work was supported by National Institutes of Health Grants DK47987 (to P. A. D.) and DK48823 and ES01247 (to N. B.). The costs of publication of this article were defrayed in part by the payment of page charges. This article must therefore be hereby marked "*advertisement*" in accordance with 18 U.S.C. Section 1734 solely to indicate this fact.

[S] The on-line version of this article (available at http://www.jbc.org) contains supplemental Fig. 1.

This work is dedicated to the memory of Wilfred R. Dawson (1927–2004).

§ To whom correspondence should be addressed: Dept. of Internal Medicine, Div. of Gastroenterology, Wake Forest University School of Medicine, Medical Center Blvd., Winston-Salem, NC 27157. Tel.: 336-716-4633; Fax: 336-716-6376; E-mail: pdawson@wfubmc.edu.

[1] The abbreviations used are: ASBT, apical sodium bile acid transporter; Endo H, endoglycosidase H; Ibabp, ileal bile acid binding protein; IRES, internal ribosome entry site; Mrp, multidrug resistance-associated protein; Ost, organic solute transporter; PNGase F, peptide *N*-glycosidase F; MDCK, Madin-Darby canine kidney; PBS, phosphate-buffered saline.

antibiotics. MDCK cells were maintained in medium B consisting of Dulbecco's modified Eagle's medium containing 1000 mg/liter D-glucose, 10% (v/v) fetal calf serum, and antibiotics.

Animals—All animal procedures were approved by the Institutional Animal Care and Use Committee. Mice were housed in plastic cages in a temperature-controlled room (22 °C) with 12-h light cycling. Animals were fed *ad libitum* a cereal-based rodent chow diet (Purina). The *Slc10a2* null mice have been described previously (3).

RNA Analyses—Total RNA was extracted from frozen tissue using TRIzol Reagent (Invitrogen) as suggested by the manufacturer. For Northern blot analysis of mouse gastrointestinal tissues, total RNA from pools of animals of the same sex and genotype was fractionated on a 1.2% (w/v) agarose gel containing 2.2 M formaldehyde and transferred to Nytran (0.45 μm; Schleicher & Schuell). For analysis of other mouse tissues, a multitissue Northern blot (FirstChoice Mouse blot 1) containing 2 μg of poly(A) RNA/lane from mixed sex, 8–10-week-old Swiss Webster mice was obtained from Ambion. The blots were hybridized with the indicated ^{32}P-labeled random hexamer-primed DNA probes, and expression levels were quantified using a 445SI phosphorimaging device (Molecular Dynamics).

For real-time PCR analysis, cDNA synthesis was initiated from 1 μg of RNA using random hexamer primers and Omniscript transcription reagents (Qiagen). For each real-time PCR reaction, cDNA synthesized from 25 ng of RNA was mixed with 2× SYBR Green PCR Master Mix (Applied Biosystems) containing 500 nM specific primers. The PCR reactions were carried out in triplicate, and the samples were analyzed on an ABI 7900 sequence detection system. The oligonucleotide primer sequences used in these experiments were: mouse Asbt, 5′-TGGGTTTCTTCCTGGCTAGACT-3′ and 5′-TGTTCTGCATTCCAGTTTCCAA-3′; mouse Ostα, 5′-TACAAGAACACCCTTTGCCC-3′ and 5′-CGAGGAATCCAGAGACCAAA-3′; mouse Ostβ, 5′-GTATTTTCGTGCAGAAGATGCG-3′ and 5′-TTTCTGTTTGCCAGGATGCTC-3′; mouse GAPDH, 5′-TGTGTCCGTCGTGGATCTGA-3′ and 5′-CCTGCTTCACCACCTTCTTGAT-3′.

Analysis of Protein Expression—Synthetic peptides corresponding to amino acids 315–329 of mouse Ostα, MYYRRKDDKVGYEAC, and 91–104 of mouse Ostβ, FLRETLISEKPDLA(C), were synthesized, coupled via their carboxyl-terminal cysteine residues to keyhole limpet hemocyanin using sulfosuccinimidyl-4-(*N*-maleimidomethyl)-cyclohexane-1-carboxylate (11) and used to immunize New Zealand White rabbits (AnaSpec, Inc.). The polyclonal rabbit anti-mouse Asbt antibody was raised against a synthetic peptide corresponding to amino acids 335–348 of the mouse Asbt and has been described previously (12). The polyclonal rabbit anti-human ASBT antibody was raised against the carboxyl-terminal 39 amino acids of human ASBT that was expressed as a glutathione *S*-transferase-ASBT fusion protein. This antibody has been used previously to measure ASBT protein expression in human ileal biopsies (13). The anti-FLAG M2 monoclonal (catalog number F3165), anti-Myc (catalog number M5546), and anti-β-actin (catalog number A5441) antibodies were obtained from Sigma.

For immunoblotting analysis of tissue extracts, intestinal segments were homogenized on ice in 250 mM sucrose, 10 mM triethanolamine-HCl (pH 7.6) in the presence of a protease inhibitor mixture (0.1 mM phenylmethylsulfonyl fluoride, 10 μg/ml pepstatin, 10 μg/ml aprotonin, 10 μg/ml leupeptin) using a Potter-Elvehjem homogenizer. After tissue fragments and nuclei were pelleted at 2500 × *g*, membranes were pelleted at 20,500 × *g*, resuspended in homogenization buffer, aliquoted, and stored at −70 °C. For immunoblotting analysis of transfected cell extracts, the cell monolayers were washed with ice-cold PBS and scraped in 1 ml of ice-cold PBS containing protease inhibitors. The cells were pelleted at 10,000 × *g* at 4 °C and stored at −70 °C. Cell extracts were prepared by lysing the cell pellets in buffer B (25 mM Tris-HCl, pH 7.4, 300 mM NaCl, 1 mM $CaCl_2$, 1% Triton X-100, 1 mM phenylmethylsulfonyl fluoride, 10 μg/ml pepstatin, 10 μg/ml aprotonin, 10 μg/ml leupeptin, and 10 mM EDTA) by repeated aspiration through a 25-gauge needle. The samples were centrifuged at 10,000 × *g* for 2 min at 4 °C, and aliquots of cell supernatants were stored at −70 °C. Samples were diluted into buffer A (15% SDS, 8 M urea, 10% (w/v) sucrose, 62.5 mM Tris-HCl, and 5 mM dithiothreitol at pH 6.8), heated at 37 °C for 30 min, and subjected to SDS-PAGE on 10 or 12% polyacrylamide gels. After transfer to nitrocellulose membranes, blots were blocked for 1 h in 5% nonfat dried milk, dissolved in blotting buffer (50 mM Tris-HCl, 80 mM NaCl, 2 mM $CaCl_2$) containing 0.2% Nonidet P-40 (NTBS). Membranes were incubated for 1 h with the primary antibody, washed in NTBS containing nonfat dry milk, and then incubated with horseradish peroxidase-conjugated second antibody (Amersham Biosciences). The following dilutions of antibodies were used: anti-Ostα or anti-Ostβ, 1:500; anti-Asbt, 1:500; anti-FLAG, 1:1000; anti-Myc, 1:1000, anti-β-actin, 1:10,000; horseradish peroxidase-conjugated anti-rabbit antibody, 1:5,000; horseradish peroxidase-conjugated anti-mouse antibody, 1:10,000. Antibody binding was then detected using an enhanced chemiluminescence technique (Amersham Biosciences).

For endoglycosidase H (Endo H) digestion, aliquots of tissue or cell extracts were incubated for 1 h at 37 °C with 1.25×10^3 units of Endo H (New England Biolabs) in 50 mM sodium citrate, pH 5.5, 0.5% SDS, and 1% β-mercaptoethanol. For peptide:*N*-glycosidase F (PNGase F) digestion, aliquots of tissue or cell extracts were incubated for 1 h at 37 °C with 1.25×10^3 units of PNGase F (New England Biolabs) in 50 mM sodium phosphate, pH 7.5, 1% Nonidet P-40, 0.5% SDS, and 1% β-mercaptoethanol. The samples were then brought to 7.5% SDS, 4 M urea, 5% (w/v) sucrose, and 2.5 mM dithiothreitol, heated for 1 h at 37 °C, and resolved by SDS-PAGE on 12% acrylamide gels. After transfer to nitrocellulose membranes, the blots were blocked and incubated with antibody as described above.

Immunolocalization (Tissue)—Mouse intestinal tissue was mounted in OCT compound (Ted Pella, Inc.), frozen in liquid nitrogen, and stored at −70 °C. Sections (6 μm) of mouse intestine were air-dried for 2 h, fixed in freshly prepared 3.7% formaldehyde/PBS, washed in PBS, and stored at 4 °C. The sections were then incubated in blocking solution (PBS containing 0.5% Tween 20 and 5% fetal calf serum) for 20 min at room temperature. The cells were fixed with freshly prepared 3.7% formaldehyde/PBS for 10 min at room temperature and then incubated in blocking solution (PBS containing 0.1% saponin and 1% bovine serum albumin) for 20 min at room temperature. The tissue sections or cells were incubated with a 1:100 dilution of anti-Ostα, Ostβ, or Asbt antibody in blocking solution for 30 min at room temperature. Samples were washed three times in PBS and then incubated with 25 μg/ml of rhodamine-conjugated goat anti-rabbit IgG secondary antibody (Jackson ImmunoResearch Laboratories) in blocking solution for 30 min at room temperature. After three washes with PBS, the sections were fixed in 3.7% formaldehyde for 10 min. Following fixation, the samples were washed three times in PBS, and nuclei were stained with 1 μg/ml TO-PRO-3 (Molecular Probes) in PBS for 10 min at room temperature. Following an additional two washes in PBS, coverslips were mounted with Vectashield HardSet mounting media (Vector Laboratories). Confocal images were obtained using a Zeiss laser scanning 510 confocal microscope equipped with a fluorescein (band pass 505–530)/rhodamine (band pass 565–615)/far red (long pass 650) filter set. For each experiment, a section or dish was incubated with the secondary antibody alone to determine background fluorescence.

Construction of Mouse Ostα and Ostβ Expression Plasmids—A mouse Ostα expression plasmid was constructed as follows. Mouse I.M.A.G.E. cDNA clone 5041102 encoding 143 nucleotides of 5′ untranslated region, the full-length 1023 nucleotide coding region, and a 205 nucleotide 3′ untranslated region was obtained from Invitrogen, and the entire cDNA insert was sequenced. A PCR-based strategy using *Pfu* polymerase (Stratagene) was employed to append the FLAG epitope (DYKDDDDK) to the carboxyl terminus of mouse Ostα. The carboxyl-terminal epitope-tagged Ostα was then subcloned into the pcDNA3.1/Hygro(+) plasmid (Invitrogen). The mouse Ostβ clone has been described previously (14). A PCR-based strategy using *Pfu* polymerase (Stratagene) was employed to append a Myc epitope (EQKLISEEDL) to the carboxyl terminus of mouse Ostβ. The carboxyl-terminal epitope-tagged Ostβ was then subcloned into the pcDNA3.1/Hygro(+) plasmid. To co-express both Ost subunits, the epitope-tagged Ostα and Ostβ cDNA inserts were sequentially cloned into the 5′ and 3′ multicloning site cassettes, respectively, of pIRES (Clontech). In pIRES, an encephalomyocarditis virus internal ribosomal entry site (IRES) mediates translational initiation from the 3′ cassette and a cytomegalovirus promoter drives expression of the bicistronic transcript. The entire expression cassette, including the epitope-tagged mouse Ostα and Ostβ cDNA inserts was removed from pIRES and subcloned into pcDNA3.1/Hygro(+) to generate a hygromycin-resistant plasmid expressing both Ost subunits. All cDNA inserts were sequenced using a PerkinElmer ABI Prism 377 sequencer. Unless otherwise indicated, the cell transfection experiments were performed using the epitope-tagged Ostα and Ostβ constructs.

Expression in Transiently Transfected HEK293 Cells—On day 0, 35-mm plates of HEK293 cells were seeded with 7.6×10^5 cells/plate. On day 1, each plate was transfected using FuGENE 6 transfection reagent (Roche Applied Science). On day 2, the cells were incubated at 37 °C with the indicated concentration of [^{3}H]taurocholate in Hanks' buffered saline solution containing 137 mM Na^+ for 10–30 min. The cells were washed in Hanks' buffered saline solution and harvested to determine cell-associated radioactivity and protein, as described previously (15).

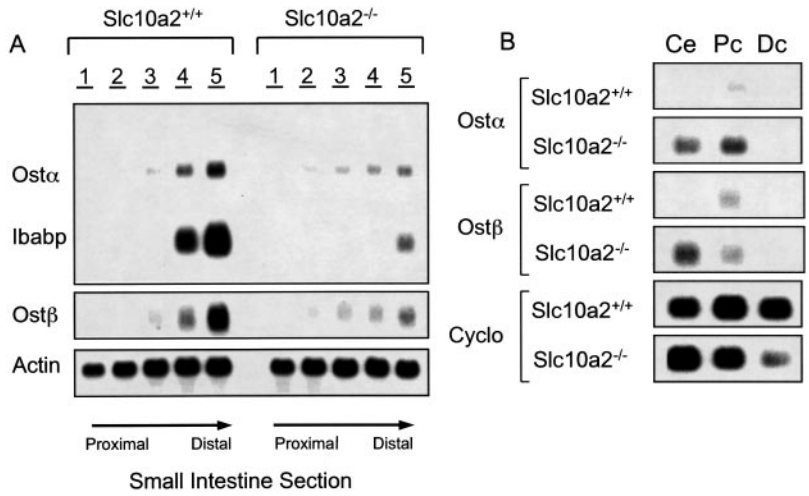

FIG. 1. **Expression of Ostα and Ostβ mRNA in wild type and *Slc10a2* null mice.** *A*, the small intestine (subdivided into five equal segments) was used to isolate total RNA. Ostα, Ostβ, Ibabp, and actin mRNA levels were then measured in pooled aliquots (5 male 129S6/SvEv mice, 4 months of age) of total RNA (10 μg) by Northern blot hybridization. *B*, pooled aliquots (3 female 129S6/SvEv mice, 7 months of age) of total RNA (10 μg) from cecum (*Ce*), proximal colon (*Pc*), and distal colon (*Dc*) were subjected to Northern blot hybridization using ^{32}P-labeled Ostα, Ostβ, or cyclophilin probes.

Transport Assays in Stably Transfected MDCK Cells—The human ASBT stably transfected MDCK cells have been described previously (16). The human ASBT and mouse Ostα-Ostβ subunits were stably expressed in MDCK cells as follows. On day 0, 100-mm plates were seeded with 1.5×10^6 MDCK-ASBT cells. On day 1, the cells were transfected with 6 μg of the mouse Ostα, Ostβ, or OstαIRESOstβ expression plasmids using the FuGENE 6 transfection reagent. On day 3, the cells were trypsinized and reseeded at 4.6×10^5 cells/plate in medium containing 350 μg/ml of G418 (Invitrogen) and 300 μg/ml of hygromycin (Invitrogen). After selection for 19–21 days, ~75 individual colonies were picked for each plasmid construct transfected, expanded in 35-mm plates, and screened by immunoblotting for Ostα and Ostβ protein expression.

For bile acid uptake and trans-cellular transport assays, stably transfected MDCK-ASBT, MDCK-ASBT/Ostα, MDCK-ASBT/Ostβ, or MDCK-ASBT/OstαIRESOstβ were plated on 24-well plates or 12-mm Transwell filter inserts (Costar) at 3×10^5 cells/well or insert. The medium in the basolateral and apical chambers was changed every 2–3 days. Formation of a tight seal between the apical and basolateral chambers was monitored by trans-epithelial transport of inulin [^{14}C]carboxylic acid (~50 μM). After incubation for 30 min at 37 °C, the diffusion of radiolabeled inulin across the cell monolayer from the apical and basolateral chambers was <1.1 and <0.2%, respectively. Following formation of the tight monolayer (typically between days 6 and 10), the cells were refed medium B containing 10 mM sodium butyrate to induce expression of the transfected genes (16). Approximately 20 h later, the cell monolayers were washed and incubated at 37 °C for 10–60 min with Hanks' buffered saline solution plus 10 μM [^{3}H]taurocholate added to the apical or basolateral chambers. Trans-cellular transport was monitored by sampling the contra-lateral chamber. After incubation, the cells were washed in ice-cold Hanks' buffered saline solution and harvested to determine cell-associated radioactivity and protein.

Statistical Analyses—Mean values ± S.D. are shown in Figs. 5, 7, and 8. The data were evaluated for statistically significant differences using the two-tailed Student's *t* test, assuming equal variance (Statview). Differences were considered statistically significant at $p < 0.05$.

RESULTS

Analysis of Transporter Gene Expression in Slc10a2$^{-/-}$ Mice—In an attempt to identify candidate basolateral bile acid transporters, the mRNA expression for a group of 180 known and orphan solute transporters was measured in the ileum, colon, and liver tissue of wild type and *Slc10a2* null mice using real-time PCR. It was hypothesized that the basolateral bile acid transporter would be highly expressed in the ileum and positively regulated by bile acids. As such, its expression would be decreased in the ileum tissue of the *Slc10a2* null mice in response to the decreased uptake of bile acids and possibly be induced in the cecum and colon tissue of these animals in response to the 10-fold increased flux of bile acids through their large intestine (3). One of the transporter genes that was significantly induced in the colon tissue of *Slc10a2* null mice was the mouse ortholog of the organic solute transporter (Ost) α subunit. Wang *et al.* (17) originally identified the Ost transporter complex (Ostα-Ostβ) from the little skate (*Leucoraja erinacea*) using expression cloning in *Xenopus* oocytes (17), and this same laboratory subsequently cloned and expressed the human and mouse orthologs of the skate Ostα-Ostβ proteins (14). Remarkably, solute transport requires the expression of two different subunits, a 340-amino acid polytopic membrane protein (Ostα) and a 128-amino acid single trans-membrane protein (Ostβ), and when co-expressed, these two proteins mediate the transport of bile acids and other sterols (14, 17). Moreover, human OSTα and OSTβ are expressed in relative abundance in tissues that also express the ASBT, namely the human small intestine, kidney, and liver (14), suggesting that OSTα-OSTβ may be a basolateral bile acid exporter. To directly test this hypothesis, the present studies examined the tissue expression, protein localization, and functional activity of mouse Ostα-Ostβ.

Northern blotting using mouse Ostα and Ostβ probes confirmed the real-time RT-PCR results obtained for Ostα and demonstrated that both Ostα and Ostβ mRNA was decreased in ileum and significantly induced in cecum and colon tissue of the *Slc10a2* null mice (Fig. 1). The expression of Ibabp mRNA, which is positively regulated by bile acids via the nuclear farnesoid X receptor (18), was used as a positive control for this study. Similar to Ostα and Ostβ, Ibabp expression was decreased in the distal small intestine (Fig. 1*A*) and induced in the cecum and colon tissue (data not shown) of the *Slc10a2* null mice. The apparent positive regulation of Ostα-Ostβ by bile acids coupled with their high ileal expression and bile acid transport potential further supported a role for Ostα-Ostβ as an ileal basolateral bile acid transporter.

Tissue Expression of Mouse Ostα and Ostβ—Northern blot analysis of multiple mouse tissues demonstrated single 1.5- and 0.8-kb transcripts for Ostα and Ostβ, respectively, in mouse kidney but not heart, brain, liver, spleen, embryo, lung, thymus, ovary, or testis (Fig. 2*A*). To examine the gastrointestinal expression of Ostα and Ostβ mRNA, Northern blot and real-time PCR analysis was performed using total RNA from mouse liver, stomach, duodenum, jejunum, ileum, cecum, proximal colon, and distal colon tissue. As shown in Fig. 2, *B* and *C*, Ostα and Ostβ mRNA expression closely parallel one another. In addition, Ostα and Ostβ mRNA expression along the cephalocaudal axis was similar to that of the Asbt, with low levels in the proximal small intestine and the highest levels in the ileum. In contrast, Mrp3 mRNA expression was highest in the colon, liver, stomach, and proximal small intestine (Fig. 2*B*). Expression of Mrp4 mRNA, another candidate bile acid efflux pump (19), was undetectable in intestine under these Northern blotting conditions. Real-time PCR analysis revealed that

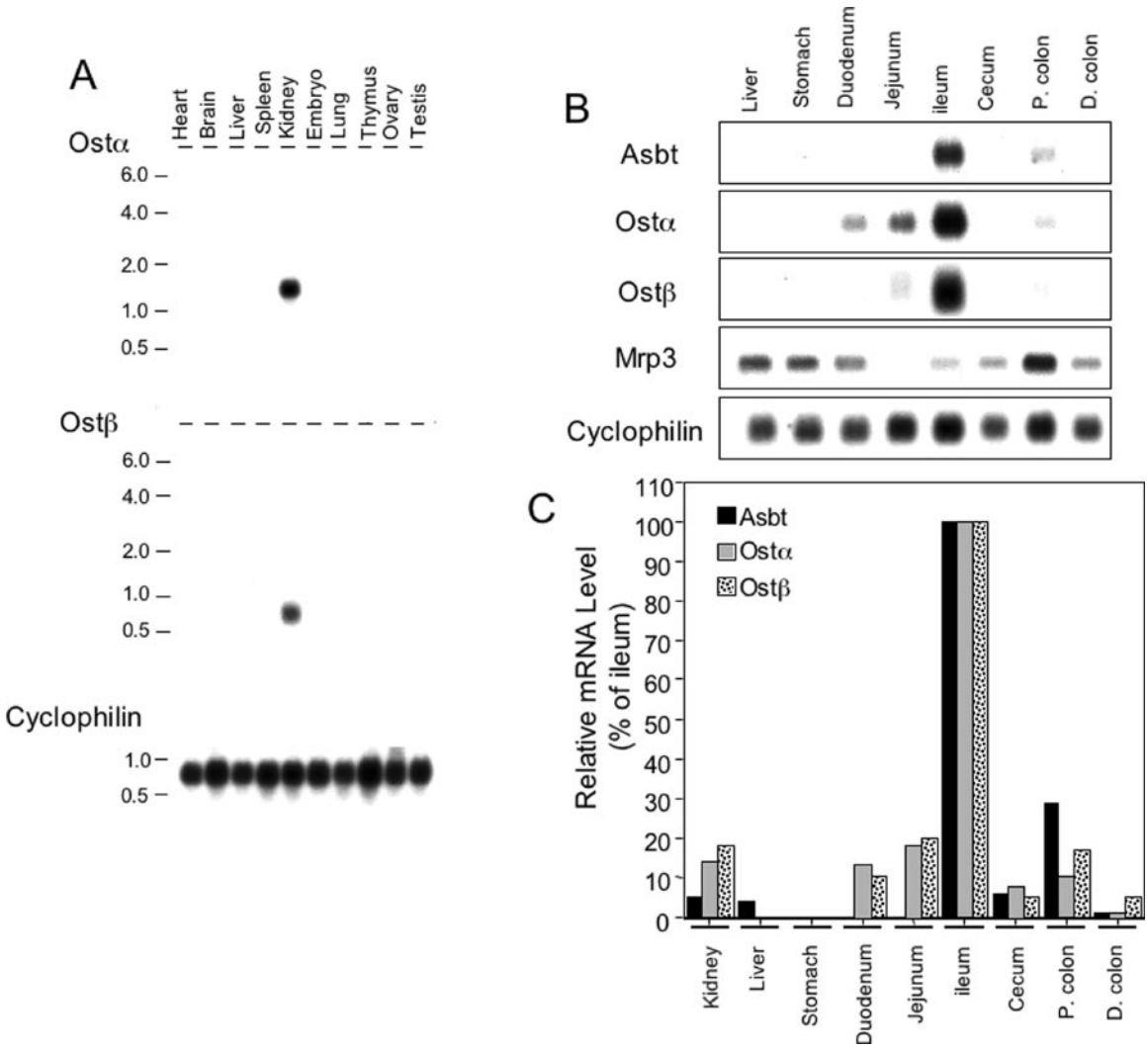

FIG. 2. **Tissue distribution of mouse Ostα and Ostβ mRNA.** *A*, tissue distribution of Ostα and Ostβ mRNA in the mouse. A blot containing 2 μg of poly(A)$^+$ mRNA from the indicated mouse tissues was hybridized with a radiolabeled probe from the Ostα (*upper panel*) or Ostβ (*lower panel*) cDNA. Control experiments with a cyclophilin probe revealed that mRNA was present in all lanes of the blot. *B*, gastrointestinal tissue distribution of Asbt, Ostα, Ostβ, and Mrp3 mRNA in the mouse. A blot containing pooled aliquots of total RNA (10 μg) (3 female 129S6/SvEv mice, 7 months of age) from the indicated tissues was hybridized to the indicated radiolabeled probes for the Asbt, Ostα, Ostβ, Mrp3, or cyclophilin cDNAs. *C*, Asbt, Ostα, and Ostβ expression in the indicated mouse tissues was determined by real-time PCR. The threshold values (C_T) are the means of triplicate determinations, and expression was normalized for GAPDH expression. The normalized threshold values are plotted as a percent of the ileal values (*% of ileum*). The threshold values determined in ileum were 19.4, 20.1, and 19.0 for Asbt, Ostα, and Ostβ, respectively.

Mrp4 mRNA is expressed at only low levels in the small intestine (data not shown).

To examine Ost protein expression, crude membranes were prepared from mouse small intestine and subjected to SDS-PAGE and immunoblotting analysis. As shown in Fig. 3*A*, the anti-Ostα antibody detected a ~40-kDa protein as well as a small amount of unresolved Ostα oligomer. Like the Asbt, Ostα protein was expressed primarily in mouse distal small intestine and at lower levels in proximal small intestine. Because the mouse Ostα sequence includes a potential *N*-linked glycosylation site, we also examined the glycosidase sensitivity of the mouse Ostα. As a positive control, Asbt was examined in the same glycosidase-treated mouse ileal membrane extracts. The mouse Asbt is a membrane glycoprotein with two *N*-linked carbohydrate chains (20). As shown in Fig. 3*B*, the mobility of Asbt and Ostα proteins was affected by treatment with PNGase F but not Endo H. The ~4-kDa change in the Ostα protein apparent molecular mass is consistent with the addition of a single mature *N*-linked carbohydrate chain.

Immunolocalization of Mouse Ostα and Ostβ to the Basolateral Domain of Mouse Ileal Enterocytes—Immunofluorescence microscopy was used to study the distribution and localization of the Asbt, Ostα, and Ostβ in mouse ileum. As shown previously (21–23), Asbt expression was restricted to the apical domain on the mature villus enterocytes with little detectable staining in the goblet cells or crypt enterocytes (Fig. 4*A*). Mouse Ostα (Fig. 4*B*) and Ostβ (Fig. 4*C*) showed a similar vertical distribution of staining along the crypt-to-villus axis, with maximal staining of the mature villus enterocytes. In contrast to the Asbt (Fig. 4*D*), Ostα (Fig. 4*E*) and Ostβ (Fig. 4*F*) were mainly localized to the lateral and basal membranes of the ileal enterocytes. Staining for a small fraction of Ostβ and Ostα protein was also detected in intracellular membranes of the enterocytes. Several controls were performed to demonstrate the specificity of the antibody staining (supplemental data, Fig. 1). No antibody reaction was observed when the ileal sections were incubated with secondary antibody alone or when mouse duodenum sections were stained with the anti-Ostα or -Ostβ antibodies.

Expression and Localization of Mouse Ostα and Ostβ in Transfected HEK293 Cells—Previous transient expression studies in *Xenopus* oocytes have focused on demonstrating that

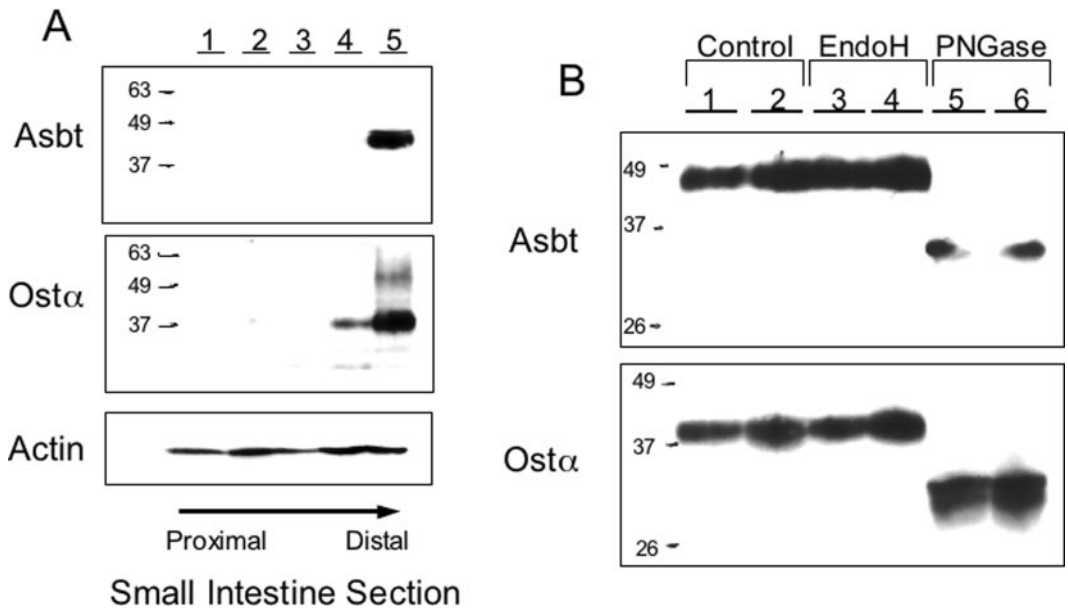

FIG. 3. **Localization of Asbt and Ostα protein in the mouse small intestine and their sensitivity to glycosidase treatment.** *A*, immunoblotting analysis of mouse small intestinal tissue segments. The small intestine was divided into five segments of equal length and used for membrane isolation. Aliquots of intestinal membrane protein (50 μg) were subjected to immunoblotting analysis using antibodies to the Asbt, Ostα, or β-actin, as indicated. *B*, glycosidase sensitivity of Asbt and Ostα. Aliquots of ileal membrane protein (50 μg) were incubated in the absence (*lanes 1* and *2*) or presence of Endo H (*lanes 3* and *4*) or PNGase F (*lanes 5* and *6*) and then subjected to immunoblotting analysis using the indicated antibodies.

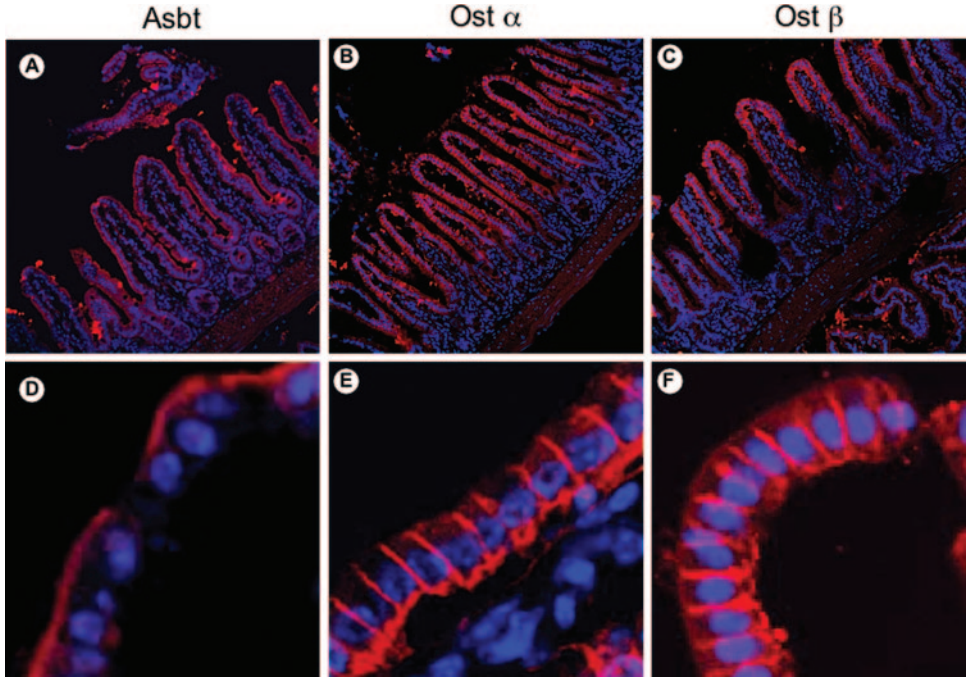

FIG. 4. **Immunolocalization of Ostα and Ostβ in mouse ileum.** Sections (6 μm) of mouse ileum were fixed with 3.7% formaldehyde/PBS, permeabilized with 0.05% Tween 20, and stained with polyclonal antibodies raised against Asbt (*A* and *D*), Ostα (*B* and *E*), or Ostβ (*C* and *F*) to determine their tissue and subcellular localization.

co-expression of both Ostα and Ostβ is required to mediate [^{3}H]taurocholate uptake (14, 17). However, is the fact that Ostα-Ostβ mediates taurocholate uptake and is still consistent with its postulated role in basolateral efflux. Previous studies have demonstrated bi-directional bile acid transport using ileal basolateral membranes (4). By functioning as a facilitative transporter or an anion exchanger, Ostα-Ostβ is predicted to move bile acids down their electrochemical gradient either into or out of the cell. Thus, the bile acid concentration gradient across the enterocyte and unidirectional nature of Asbt transport would promote Ostα/β-mediated bile acid export across the basolateral membrane *in vivo*.

To better understand the functional requirement for the two subunits in mammalian cells, the taurocholate uptake activity, protein expression, and cellular localization was examined for Ostα-Ostβ in transfected HEK293 cells. As shown in *Xenopus* oocytes (14, 17), co-expression of Ostα and Ostβ stimulated taurocholate transport over the background levels exhibited by the individual subunits (Fig. 5*A*). In addition, taurocholate uptake was similar in HEK293 cells transfected with either the

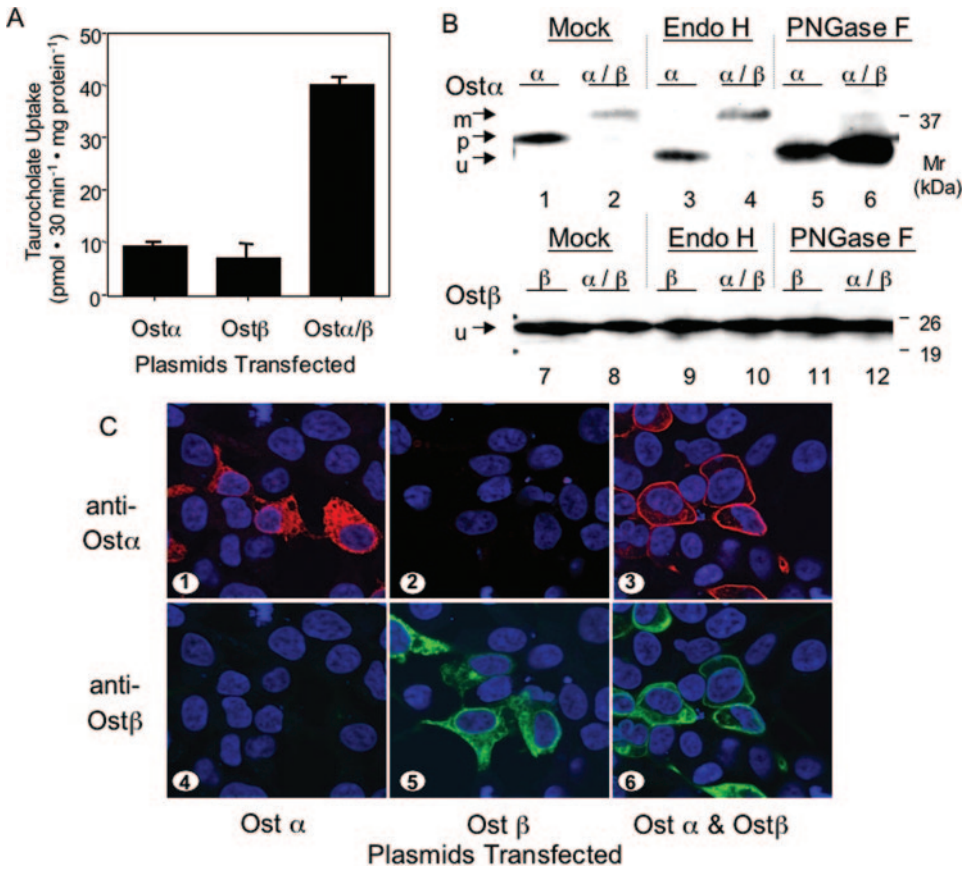

FIG. 5. **Expression, functional activity and glycosidase sensitivity of Ostα and Ostβ in HEK293 cells**. *A*, on day 0, HEK293 cells were seeded in 35-mm dishes. On day 1, the cells were transfected with β-galactosidase, Ostα, Ostβ, or Ostα-Ostβ. On day 2, the cells were washed and incubated in Hanks' buffered saline containing 25 μM [^{3}H]taurocholate for 30 min at 37 °C. Cells were then washed and lysed to determine cell-associated radioactivity and protein. The uptake is expressed as pmol of taurocholate transported/mg of protein (mean ± S.D., $n = 3$) and is corrected for the background uptake in β-galactosidase transfected cells (15.6 ± 0.6). Taurocholate uptake was significantly increased following co-transfection with Ostα plus Ostβ ($p < 0.001$). *B*, on day 0, HEK293 cells were seeded in 60-mm dishes. On day 1, the cells were transfected with Ostα, Ostβ, or Ostα-Ostβ. On day 2, the cells were lysed, and 100 μg of cell protein was incubated in the absence (*lanes 1, 2, 7, 8*) or presence of Endo H (*lanes 3, 4, 9, 10*), or PNGase F (*lanes 5, 6, 11, 12*). Samples were then subjected to immunoblotting analysis for Ostα (*lanes 1–6*) and Ostβ (*lanes 7–12*). The migration of the precursor (*p*), mature glycosylated (*m*), and unglycosylated (*u*) forms are indicated. *C*, on day 0, HEK293 cells were seeded onto glass coverslips. On day 1, the cells were transfected with Ostα (*panels 1* and *4*), Ostβ (*panels 2* and *5*), or Ostα-Ostβ (*panels 3* and *6*). After 24 h, the cells were fixed with 3.7% formaldehyde/PBS and permeabilized using a solution of 1% bovine serum albumin and 0.1% saponin in PBS. The cells were then stained with mouse M2 anti-FLAG to detect Ostα (*red*), rabbit polyclonal anti-Ostβ (*green*), and To-Pro-3 (*blue*) to visualize nuclei and then viewed using laser scanning confocal microscopy.

wild type or epitope-tagged Ostα-Ostβ subunits, indicating that the epitope tags did not alter transport function (data not shown). When expressed alone, Ostα migrated upon SDS-PAGE as a single band with a smaller apparent mass than observed in mouse ileum (~35 *versus* 40 kDa) (Fig. 5*B*, *lane 1*). However when co-expressed with Ostβ, Ostα migrated as a single band with an apparent molecular mass of ~40 kDa (Fig. 5*B*, *lane 2*). Because these different molecular mass values may reflect differences in *N*-linked glycosylation, we examined the glycosidase sensitivity of the two Ostα forms. Most *N*-glycans on glycoproteins that transit the Golgi complex during delivery to the cell surface are modified from an immature high mannose precursor to a mature complex form by a series of enzymatic steps (24). One distinguishing feature for these two types of *N*-glycans is their sensitivity to digestion with Endo H. In general, *N*-glycans on proteins prior to their delivery to the medial Golgi complex are substrates for Endo H, whereas *N*-glycans on proteins after this point in the secretory pathway are not substrates due to processing by *N*-acetylglucosaminyltransferase I and mannosidase II. PNGase F, by contrast, cleaves *N*-glycans from glycoproteins regardless of their localization along the secretory pathway (25). When co-expressed with Ostβ, the Ostα *N*-linked carbohydrate was processed to an Endo H-resistant form (Fig. 5*B*, *lanes 3–6*), indicating that Ostα had exited the endoplasmic reticulum and trafficked through the Golgi complex. There was no change in the apparent molecular weight of Ostβ regardless of whether it was co-expressed with Ostα (Fig. 5*B*, *lanes 7–12*). Although mouse Ostβ also encodes a potential *N*-linked glycosylation site at amino acid position 33, this site lies within a predicted transmembrane domain and does not appear to be utilized. To confirm that changes in Ostα glycosylation correlated with changes in cellular localization, indirect immunofluorescence and confocal microscopy was performed. When expressed alone, Ostα displayed an endoplasmic reticulum-staining pattern with little detectable plasma membrane staining (Fig. 5*C*, *panel 1*). However when co-expressed with Ostβ, Ostα was localized primarily on the plasma membrane (Fig. 5*C*, *panel 3*). Similar results were obtained for Ostβ, except that there was also a small amount of Golgi and plasma membrane staining when Ostβ was expressed alone (Fig. 5*C*, *panel 5*). When co-expressed with Ostα, the plasma membrane staining for Ostβ was dramatically increased (Fig. 5*C*, *panel 6*).

Bile Acid Transport in Triply Transfected MDCK Cells Expressing Ostα, Ostβ, and ASBT—The ability of Ostα-Ostβ to function as a basolateral bile acid efflux transporter was examined in triply transfected MDCK cells expressing the ASBT, Ostα, and Ostβ. For this study, the expression of Ostα and Ostβ

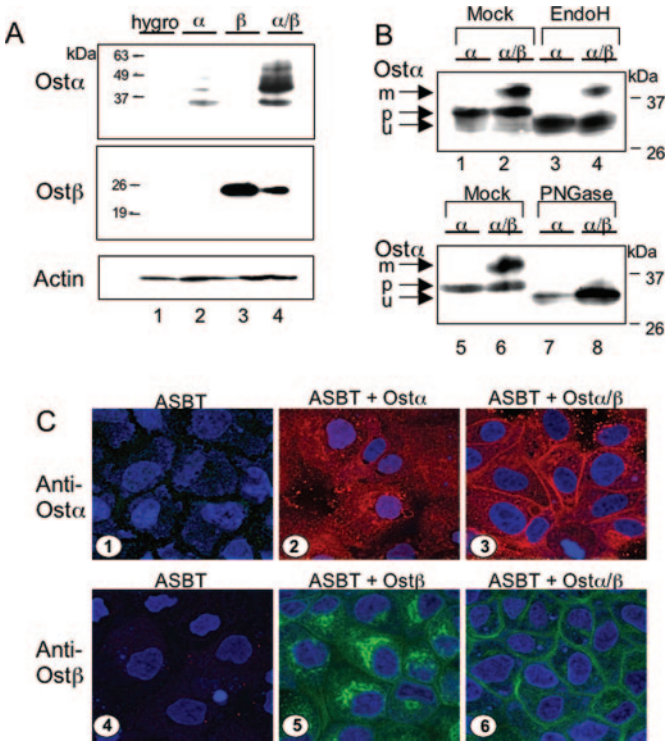

FIG. 6. **Expression and glycosidase sensitivity of Ostα and Ostβ in stably transfected MDCK cells.** *A*, MDCK-ASBT cells stably transfected with the indicated plasmids were lysed, and 100 μg of cell protein was subjected to immunoblotting analysis for Ostα, Ostβ, and β-actin, as indicated. *B*, MDCK-ASBT cells stably transfected with Ostα (α) or Ostα-Ostβ (α/β) were lysed, and 100 μg of cell protein was incubated in the absence (*lanes 1, 2, 5, 6*) or presence (*lanes 3, 4*) of Endo H or PNGase F (*lanes 7, 8*). Samples were then subjected to immunoblotting analysis for Ostα. *C*, MDCK-ASBT cells stably transfected with pHygro (*panels 1* and *4*), Ostα (*panels 2* and *5*), or OstαIRESOstβ (*panels 3* and *6*) were seeded onto glass coverslips. After 24 h, the cells were fixed with 3.7% formaldehyde/PBS and permeabilized using a solution of 1% bovine serum albumin and 0.1% saponin in PBS. The cells were then stained with rabbit polyclonal anti-Ostα (*red*, *panels 1–3*), rabbit polyclonal anti-Ostβ (*green*, *panels 4–6*) and To-Pro-3 (*blue*) to detect nuclei and then viewed using laser scanning confocal microscopy.

was first analyzed by immunoblotting (Fig. 6, *A* and *B*). In agreement with the results obtained with the transiently transfected HEK293 cells (Fig. 5*B*), a portion of the Ostα protein shifted to a higher molecular form that was Endo H-resistant and PNGase-sensitive when co-expressed with Ostβ in the MDCK cells (Fig. 6*B*). This shift correlated with changes in the subcellular location of Ostα, such that significant plasma membrane staining could then be observed (Fig. 6*C*, *panel 3*). Ostβ also showed changes in cellular localization, going from primarily a Golgi staining pattern (Fig. 6*C*, *panel 5*) to plasma membrane (Fig. 6*C*, *panel 6*). Note that the relative amount of mature Ostα protein was lower in the stably transfected MDCK cells than in the transiently transfected HEK293 cells, perhaps due to a limiting amount of Ostβ protein expression (Fig. 6*A*). Both Ostα and Ostβ are expressed from a single bicistronic transcript in the MDCK cells, and it has been noted previously that IRES-dependent gene expression is lower than 5′ cap-dependent gene expression in a bicistronic vector (26).

The bile acid uptake properties of the MDCK/ASBT cells transfected with the various Ost constructs are shown in Fig. 7. The MDCK/ASBT cell lines all exhibited similar levels of sodium-dependent bile acid uptake (Fig. 7*A*), reflecting similar levels of ASBT protein expression (data not shown). As shown in previous expression studies using *Xenopus* oocytes (14, 17) and the transiently transfected HEK293 cells (Fig. 5*A*), co-expression of Ostα and Ostβ was required to stimulate Na^+-independent taurocholate uptake over the background levels exhibited by the individual subunits (Fig. 7*B*).

To examine the ability of Ostα-Ostβ to function as a basolateral bile acid efflux transporter, the transfected MDCK/ASBT cells expressing Ostα, Ostβ, or Ostα-Ostβ were grown on Transwell filter inserts and assayed for their ability to mediate trans-cellular transport. The MDCK/ASBT cells expressing Ostα or Ostβ alone exhibited only background levels of apical to basolateral taurocholate trans-cellular transport, whereas cells expressing both Ost subunits mediated significant taurocholate trans-cellular transport (Fig. 8). In contrast to the apical transport, expression of Ostα-Ostβ had no effect on the basolateral to apical trans-cellular transport of taurocholate (Fig. 8, *inset*), reflecting the appropriate sorting of the proteins, the unidirectional nature of the ASBT-mediated apical transport, and the apparent absence of other apical taurocholate transporters.

DISCUSSION

Intestinal absorption of bile acids in many vertebrate species, including humans, occurs primarily in the terminal ileum (1). Although the Asbt mediates bile acid uptake across the apical brush-border membrane of ileal enterocytes, the proteins responsible for bile acid export across the basolateral membranes of these cells have not been identified. Previous *in vitro* studies using rat ileal basolateral membrane vesicles have demonstrated bile acid anion exchange (4) as well as ATP-dependent bile acid transport activity (27). However, the relative *in vivo* contribution of these transport activities to basolateral bile acid export is unknown. Several different candidate genes have also been proposed for the ileal basolateral transporter, including the ABC transporter Mrp3 (9, 10) and an alternatively spliced form of the Asbt (8). Unfortunately, their roles in ileal basolateral bile acid transport remain uncertain. The major finding of this study is the identification of Ostα-Ostβ as a major basolateral bile acid transporter in ileum, where it may play an important role in the regulation of bile acid and sterol homeostasis.

A transcriptional profiling approach was employed to identify additional candidate intestinal basolateral bile acid transporters. It was hypothesized that the basolateral transporter would be highly expressed in ileum and positively regulated by bile acids. As such, its expression would be decreased in ileum and increased in the colon of *Slc10a2* null mice, a model of ileal bile acid malabsorption (3). One of the most highly expressed and regulated genes identified in this analysis was the mouse Ostα subunit of the Ostα-Ostβ transporter complex. As summarized below, the OSTα-OSTβ transporter displays several remarkable features. OST-mediated transport requires the co-expression of two distinct gene products, a 340-amino acid, 7-potential trans-membrane domain protein (OSTα) and a 128-amino acid, single trans-membrane domain ancillary polypeptide (OSTβ). The predicted amino acid sequences for OSTα and OSTβ are novel and are not homologous to any previously identified solute carrier gene family, indicating a new type of membrane transporter (14, 17). Moreover, the mouse and human OST proteins are able to complement each other, as well as those from the skate, indicating a high degree of functional conservation throughout evolution (14). Of significance for the present study, OSTα-OSTβ have been shown to transport taurocholate in addition to other sterols (estrone 3-sulfate, dehydroepiandrosterone 3-sulfate, and digoxin), and prostaglandin E_2 (14, 17) and OSTα-OSTβ mRNAs are expressed in a variety of human tissues, with the highest levels occurring in the small intestine, kidney, and liver, the same tissues that express the ASBT (14). Thus, these expression and transport properties of

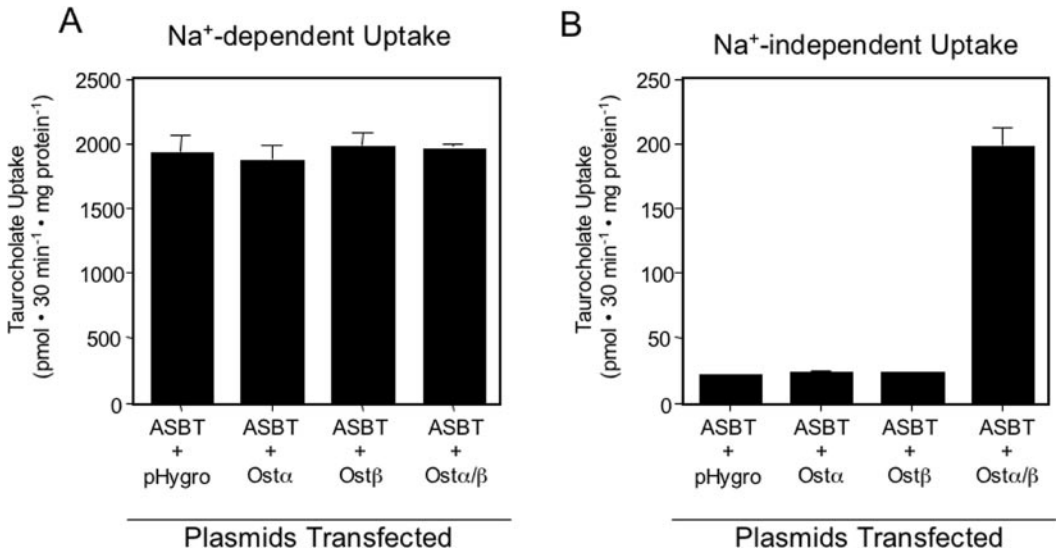

FIG. 7. **Bile acid uptake activity in stably transfected MDCK cells.** On day 0, MDCK cells stably transfected with the indicated plasmids were seeded onto 24-well plates. On day 2, expression of the transfected plasmids was induced by the addition of 10 mM sodium butyrate. After 20 h, the cell monolayers were washed and incubated for 30 min at 37 °C with 10 μM [^{3}H]taurocholate either in the presence of 137 mM Na^+ (*A*) or K^+ (*B*). The cells were then washed and processed to determine cell-associated protein and radioactivity. Uptake values (mean ± S.D.) are expressed as pmol of taurocholate/mg of cell protein.

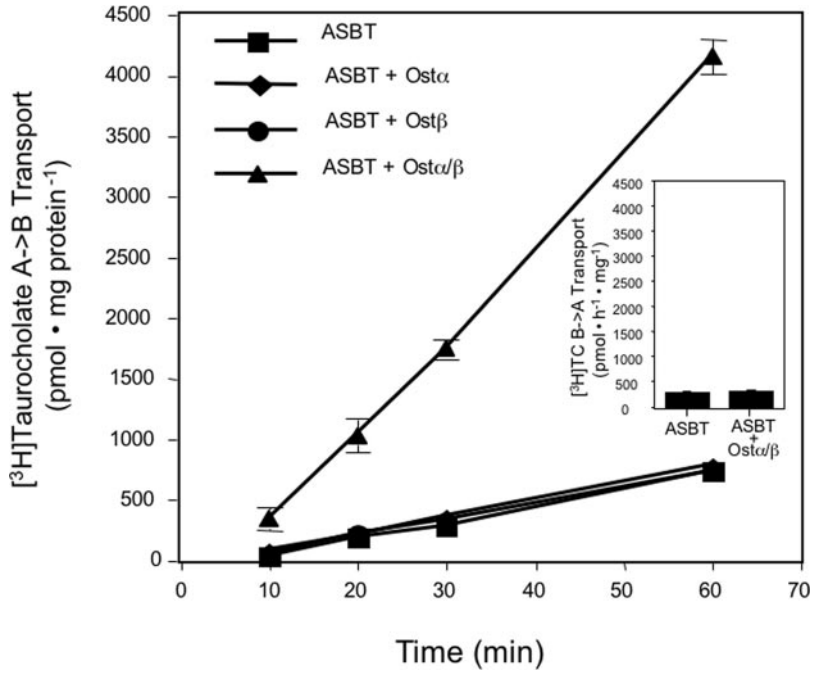

FIG. 8. **Trans-cellular transport of taurocholate in stably transfected MDCK cells.** MDCK cells transfected with the indicated plasmids were plated onto Transwell filter inserts on day 0. Expression of the transfected plasmids was induced by the addition of 10 mM sodium butyrate on day 7. On day 8, either the apical or the basolateral Transwell chamber received 10 μM [^{3}H]taurocholate, and aliquots of media in the opposite chamber were sampled over 60 min. Data for the apical to basolateral transport are shown in the *line graph*. Data for basolateral to apical transport after 60 min are shown in the *inset*. Values are means ± S.D., $n = 3$.

OSTα-OSTβ were consistent with a potential role as a major basolateral bile acid transporter.

Strong support for a role of Ostα-Ostβ in basolateral bile acid transport was provided by the tissue expression and localization studies. These data demonstrated that Ostα and Ostβ are co-expressed, and co-localize on the basolateral membrane of the same enterocytes that express the Asbt. Ostα-Ostβ and the Asbt showed a similar vertical gradient of expression along the intestinal crypt-to-villus axis with highest levels in the mature villus enterocytes and no expression in goblet cells or in the crypt enterocytes. Additional evidence suggesting that Ostα-Ostβ is a basolateral efflux carrier was provided by studies in polarized MDCK cells co-expressing mouse Ostα-Ostβ and human ASBT. When co-expressed, Ostα-Ostβ was able to support apical-to-basolateral transport of taurocholate as well as other major taurine- and glycine-conjugated bile acids (data not shown). Conversely, Ostα-Ostβ was unable to stimulate transport in the opposite direction across the cell monolayer, indicating that the Ost transporter is localized to the basolateral membrane of transfected MDCK cells and mediates bile acid efflux into the basal compartment. These results contrast with previous attempts to reproduce ileocyte trans-cellular transport in MDCK cells co-transfected with the mouse Asbt and human MRP3 (28). In those doubly transfected cells, there was insufficient MRP3-mediated basolateral bile acid transport to achieve trans-cellular transport above the endogenous MDCK cell background. Based on these studies and the apparent low affinity of MRP3 for bile acids, it was concluded that MRP3 is unlikely to be the principal ileal basolateral bile acid transporter (28).

The other major finding of this study provides insight into the mechanism by which the two subunits of this heteromeric complex interact to generate a functional transporter. A previous study in *Xenopus* oocytes demonstrated that human OSTα

and OSTβ can reach the oocyte plasma membrane when expressed individually (14), suggesting that co-expression may not be required for proper membrane targeting. However, there are several other possible interpretations of this observation, including co-trafficking of OSTα and OSTβ with endogenous oocyte proteins or mistargeting of a small fraction of the oocyte-expressed OSTα and OSTβ proteins (14). The present studies clearly demonstrated that co-expression of Ostα and Ostβ is required for delivery of the individual proteins to the plasma membrane of transfected HEK293 cells or MDCK cells. Co-expression of Ostα and Ostβ was required to convert the Ostα subunit to a mature *N*-glycosylated Endo H-resistant form, suggesting that co-expression facilitates the movement of Ostα through the Golgi apparatus. This conclusion was also supported by immunolocalization studies that showed co-expression is necessary for plasma membrane expression of Ostα and Ostβ in these cells. Stable association of both subunits may be required for transporter function. Alternatively, the Ostβ subunit may function as a chaperone to promote the egress of Ostα and possibly other proteins from the endoplasmic reticulum. Additional studies are needed to define the mechanism by which these two proteins interact, their individual roles in generating a functional complex at the plasma membrane, and their roles in solute transport.

In conclusion, the results of these studies indicate that Ostα-Ostβ is an ileal basolateral bile acid transporter. The properties of Ostα-Ostβ suggest that this is a major mechanism for ileal basolateral bile acid transport, an important missing link in our understanding of the enterohepatic circulation of bile acids.

Acknowledgments—We thank Jin-Young Lee for assistance with antibody development and characterization and Dr. Greg Shelness for critical reading of the manuscript.

REFERENCES

1. Shneider, B. L. (2001) *J. Pediatr. Gastroenterol. Nutr.* **32,** 407–417
2. Oelkers, P., Kirby, L. C., Heubi, J. E., and Dawson, P. A. (1997) *J. Clin. Investig.* **99,** 1880–1887
3. Dawson, P. A., Haywood, J., Craddock, A. L., Wilson, M., Tietjen, M., Kluckman, K., Maeda, N., and Parks, J. S. (2003) *J. Biol. Chem.* **278,** 33920–33927
4. Weinberg, S. L., Burckhardt, G., and Wilson, F. A. (1986) *J. Clin. Investig.* **78,** 44–50
5. Lin, M. C., Weinberg, S. L., Kramer, W., Burckhardt, G., and Wilson, F. A. (1988) *J. Membr. Biol.* **106,** 1–11
6. Lin, M. C., Kramer, W., and Wilson, F. A. (1990) *J. Biol. Chem.* **265,** 14986–14995
7. Lin, M. C., Mullady, E., and Wilson, F. A. (1993) *Am. J. Physiol.* **265,** G56–G62
8. Lazaridis, K. N., Tietz, P., Wu, T., Kip, S., Dawson, P. A., and LaRusso, N. F. (2000) *Proc. Natl. Acad. Sci. U. S. A.* **97,** 11092–11097
9. Hirohashi, T., Suzuki, H., Takikawa, H., and Sugiyama, Y. (2000) *J. Biol. Chem.* **275,** 2905–2910
10. Zeng, H., Liu, G., Rea, P. A., and Kruh, G. D. (2000) *Cancer Res.* **60,** 4779–4784
11. Adrian, T. E. (1997) *Methods Mol. Biol.* **73,** 239–249
12. Wong, M. H., Oelkers, P., and Dawson, P. A. (1995) *J. Biol. Chem.* **270,** 27228–27234
13. Jung, D., Fantin, A. C., Scheurer, U., Fried, M., and Kullak-Ublick, G. A. (2004) *Gut* **53,** 78–84
14. Seward, D. J., Koh, A. S., Boyer, J. L., and Ballatori, N. (2003) *J. Biol. Chem.* **278,** 27473–27482
15. Craddock, A. L., Love, M. W., Daniel, R. W., Kirby, L. C., Walters, H. C., Wong, M. H., and Dawson, P. A. (1998) *Am. J. Physiol.* **274,** G157–G169
16. Walters, H. C., Craddock, A. L., Fusegawa, H., Willingham, M. C., and Dawson, P. A. (2000) *Am. J. Physiol.* **279,** G1188–G1200
17. Wang, W., Seward, D. J., Li, L., Boyer, J. L., and Ballatori, N. (2001) *Proc. Natl. Acad. Sci. U. S. A.* **98,** 9431–9436
18. Grober, J., Zaghini, I., Fujii, H., Jones, S. A., Kliewer, S. A., Willson, T. M., Ono, T., and Besnard, P. (1999) *J. Biol. Chem.* **274,** 29749–29754
19. Rius, M., Nies, A. T., Hummel-Eisenbeiss, J., Jedlitschky, G., and Keppler, D. (2003) *Hepatology* **38,** 374–384
20. Hallen, S., Bjorquist, A., Ostlund-Lindqvist, A. M., and Sachs, G. (2002) *Biochemistry* **41,** 14916–14924
21. Shneider, B. L., Dawson, P. A., Christie, D. M., Hardikar, W., Wong, M. H., and Suchy, F. J. (1995) *J. Clin. Investig.* **95,** 745–754
22. Stelzner, M., Hoagland, V., and Somasundaram, S. (2000) *Pfluegers Arch* **440,** 157–162
23. Hakansson, P., Andersson, I., Nystrom, S., Lofgren, L., Amrot, L. F., and Li, H. (2002) *Scand. J. Gastroenterol.* **37,** 1089–1096
24. Helenius, A., and Aebi, M. (2001) *Science* **291,** 2364–2369
25. Tarentino, A. L., and Plummer, T. H., Jr. (1994) *Methods Enzymol.* **230,** 44–57
26. Mizuguchi, H., Xu, Z., Ishii-Watabe, A., Uchida, E., and Hayakawa, T. (2000) *Mol. Ther.* **1,** 376–382
27. Shoji, T., Suzuki, H., Kusuhara, H., Watanabe, Y., Sakamoto, S., and Sugiyama, Y. (2004) *Am. J. Physiol.* **284,** G749–G756
28. Zelcer, N., Saeki, T., Bot, I., Kuil, A., and Borst, P. (2003) *Biochem. J.* **369,** 23–30